RESEARCH ARTICLE

Human pulmonary microvascular endothelial cells respond to DAMPs from injured renal tubular cells

Sean E. DeWolf[1,2] | Alana A. Hawkes[2] | Sunil M. Kurian[3,4] |
Diana E. Gorial[2] | Mark L. Hepokoski[1,5] | Stephanie S. Almeida[2] |
Isabella R. Posner[2] | Dianne B. McKay[2,4]

[1]Department of Pulmonary and Critical Care Medicine, University of California San Diego, San Diego, California, USA

[2]Department of Immunology, The Scripps Research Institute, La Jolla, California, USA

[3]Scripps Clinic Bio-Repository & Bio-Informatics Core, Scripps Health, La Jolla, California, USA

[4]Department of Surgery, Scripps Clinic and Green Hospital, La Jolla, California, USA

[5]Department of Pulmonary and Critical Care Medicine, Veterans Administration, San Diego, California, USA

Correspondence
Sean E. DeWolf, 10550 North Torrey Pines Rd, Immunology room 303. Mail code IMM-8, La Jolla, CA 92037, USA.
Email: sedewolf@health.ucsd.edu

Abstract

Acute kidney injury (AKI) causes distant organ dysfunction through yet unknown mechanisms, leading to multiorgan failure and death. The lungs are one of the most common extrarenal organs affected by AKI, and combined lung and kidney injury has a mortality as high as 60%–80%. One mechanism that has been implicated in lung injury after AKI involves molecules released from injured kidney cells (DAMPs, or damage-associated molecular patterns) that promote a noninfectious inflammatory response by binding to pattern recognition receptors (PRRs) constitutively expressed on the pulmonary endothelium. To date there are limited data investigating the role of PRRs and DAMPs in the pulmonary endothelial response to AKI. Understanding these mechanisms holds great promise for therapeutics aimed at ameliorating the devastating effects of AKI. In this study, we stimulate primary human microvascular endothelial cells with DAMPs derived from injured primary renal tubular epithelial cells (RTECs) as an ex-vivo model of lung injury following AKI. We show that DAMPs derived from injured RTECs cause activation of Toll-Like Receptor and NOD-Like Receptor signaling pathways as well as increase human primary pulmonary microvascular endothelial cell (HMVEC) cytokine production, cell signaling activation, and permeability. We further show that cytokine production in HMVECs in response to DAMPs derived from RTECs is reduced by the inhibition of NOD1 and NOD2, which may have implications for future therapeutics. This paper adds to our understanding of PRR expression and function in pulmonary HMVECs and provides a foundation for future work aimed at developing therapeutic strategies to prevent lung injury following AKI.

KEYWORDS
innate immunity, pulmonary endothelium, vascular inflammation/leak

---

INTRODUCTION

Acute kidney injury (AKI) causes distant organ dysfunction through yet unknown mechanisms, leading to multiorgan failure and death. The lungs are one of the most common extrarenal organs affected by AKI,[1–3] and combined lung and kidney injury has a mortality between 60% and 80%.[4–6] The mechanisms leading to lung injury after AKI are poorly understood and represent a potential avenue for new therapeutics aimed at ameliorating the devastating effects of AKI.

One mechanism that has been recognized to play a role in kidney/lung cross-talk involves molecules released from injured kidney cells (DAMPs, or damage-associated molecular patterns). DAMPs promote a sterile inflammatory response in the lung by binding to pattern recognition receptors (PRRs) constitutively expressed in the pulmonary endothelium.[7–15] We recently showed that DAMPs generated from injured renal tubular epithelial cells (RTECs) cause upregulation of PRRs, increase production of inflammatory mediators, and activate pro-inflammatory signaling pathways in healthy renal tubular epithelium.[16] DAMPs, which contribute to injurious inflammation after renal ischemia–reperfusion injury (IRI), are likely released into the circulation where they encounter PRRs constitutively expressed in pulmonary endothelium. Binding of DAMPs to PRRs is thought to propagate inflammatory injury and cell death in the lung,[7,17–22] leading to pulmonary edema and respiratory failure.

Animal studies have demonstrated that HMGBI, a well-characterized DAMP, is increased in the circulation after AKI, and blockade of HMGB1 can reduce pulmonary inflammation following experimental AKI.[7] Despite these important advances, a more detailed understanding of PRR expression, function, and response to DAMPs in human pulmonary microvascular endothelial cells is needed. In the current study, we focus on NOD1, NOD2, NLRP3, Toll-Like Receptor (TLR)2, and TLR4 as we and others have shown that these PRRs are critical to AKI after renal IRI.[23–28] We postulate that these PRRs might also provide an important link in our understanding of kidney–lung crosstalk.

METHODS

Cells and cell culture

Human primary pulmonary microvascular endothelial cells (HMVECs) were obtained from two sources-purchased from Lonza and isolated in house from human lungs not used for transplantation. The HMVECs were grown in EBM-2 basal media (CC-3156; Lonza) with the addition of Microvascular Endothelial Cell Growth Medium SingleQuots supplements (CC-4147; Lonza). Cells were passed at 1:5 dilution and used between passage number 2–6 for all experiments.

Primary pulmonary HMVEC isolation from human lung in house was performed according to previously published methods.[29,30] The lungs used for research were provided by our local organ bank, LifeSharing™. They were discarded/not eligible for transplant, and were deidentified, thus not subject to Institutional Review Board review (per National Institute of Health Human Subjects guidelines). All lungs were tested for pathogens by nucleic acid testing per organ bank protocol. Any lungs found harboring pathogens or any public health service high-risk donors were not used. The pulmonary arteries of the donor lungs were flushed with 2 L of 50 units/mL of heparin diluted in saline intraoperatively. The lungs were then stored in 2 L of ice cold Servator P (Global Transplant Solutions) until time of dissection. After removal of the visceral pleura, 1–2 cm sections of peripheral lung tissue were removed and placed in 10 mL of ice cold M199 solution. The lung tissue was minced using scissors and digested in enzyme solution (2 mg/mL collagenase I, 0.6 units/mL dispase, 50 units/mL DNase, 10 µg/mL vancomycin/meropenem, 2.5 µg/mL amphotericin in M199 media) for 1 h at 37°C and 5% CO_2. Every 15 min, cells were passed up and down through a 16 G then 18 G needle to break up cell clumps. Cells were washed with 10 mL 10% fetal bovine serum (FBS) in M199 and strained through a 100 µm filter. Cells were then washed with 10% FBS in M199 x2 and strained through a 70-µm filter. The cells were then resuspended in 1 mL of buffer 3 (1% FBS, 1 mM $CaCl_2$, 5 mM $MgCl_2$), and magnetic bead isolation carried out using the Cellection Biotin Binder Kit (Invitrogen) according to manufacturers instructions. Antihuman CD31 antibody (clone O92E4) was obtained from BioLegend. Cells were plated into 35 mm biocoat plates in prewarmed (37°C) growth media and grown to 70% confluency. A second round of purification was then performed using the Cellection Biotin Binder Kit (Invitrogen) and the same anti-CD31 magnetic beads. To confirm the pulmonary HMVEC phenotype, FACS was performed and showed that cells were >95% pure based on cell surface staining (CD31$^+$ VEcadherin$^+$ GSL1$^+$ Carbonic Anhydrase 4$^+$).[31,32]

Human primary RTECs were isolated from human kidneys not used for transplantation. The kidneys used for research were provided by our local organ bank, LifeSharing™, were discarded, and deidentified, thus not subject to Institutional Review Board review (per

National Institute of Health Human Subjects guidelines). All kidneys were tested for pathogens by nucleic acid testing per organ bank protocol. Any kidneys found harboring pathogens or any public health service high-risk kidneys were not used. Following procurement, the kidneys were transported to the laboratory in University of Wisconsin preservative solution (Bridge to Life) at 4°C and processed immediately. The RTECs were isolated using our published methods.[27,28] Briefly, the cortex was dissected under aseptic conditions and minced, and the slurry was suspended in 1 mg/mL solution of sterile collagenase (Sigma-Aldrich). Cells were then strained through a 100-μm filter (Fisher Scientific), and RTECs were isolated by Percoll gradient centrifugation. RTE phenotype was confirmed by FACS (CD133+, AQP1+, and CA4+).

RTECs were cultured on collagen-coated Biocoat plates (Becton Dickinson) in Dulbecco's Modified Eagle Medium (DMEM):F12 + glutamine + HEPES (Gibco) with the addition of 1% v/v insulin, transferrin, selenium (Invitrogen), 0.05 μM hydrocortisone (Sigma-Aldrich), 20 ng/mL epidermal growth factor (Sigma-Aldrich), 32 ng/mL triiodothyronine (Sigma-Aldrich), and 0.5% heat-inactivated fetal bovine serum (Genesee Scientific).

Generation of necrotic supernatant from renal tubular epithelial cells

Necrotic supernatant from injured renal tubular epithelial cells was prepared as has been described in our previous work.[16] RTECs were stimulated with 0.1 mM hypoxanthine (Sigma) and 2.5 mU/mL of xanthine oxidase (Sigma) in RPMI for 2 h, washed three times with 30 mL sterile phosphate-buffered saline (PBS) and then resuspended in EBM-2 basal media (Lonza) at a concentration of 10^6 cells/100 μL media. The cell mixture was then transferred to a sterile Eppendorf tube and frozen at −80°C. The cells were then freeze-thawed overnight three times and then vortexed to cause membrane rupture and release of intracellular DAMPs. The cell debris was then removed by centrifugation at 17,000g for 30 s and the supernatant transferred to a fresh Eppendorf tube. The supernatant was tested for protein content and diluted with fresh EBM-2 media to a concentration of 1 mg/mL total protein. A frozen EBM-2 control was used by adding equal volumes of EBM-2 media to an Eppendorf tube and freeze thawing three times. An additional control was performed in preliminary experiments where we used media that had been incubated with healthy hRTE to stimulate HMVEC. This supernatant was used to control for any secreted factors from hRTE under physiologic conditions (see Supporting Information S2: Figure 1).

Mass spectrometry

Necrotic supernatant from injured RTECs was prepared as above and 100 μg of total protein added to 400 μL of 1:1 methanol:acetonitrile. Protein mixture was placed at 4°C overnight, then spun down at 17,500g for 10 min and supernatant removed. Protein was then analyzed using tandem mass spectrometry (MS/MS) on the ESI-TRAP instrument. The MASCOT search results based on protein family summary were assessed and the filters used for the search were a significance threshold of $p < 0.05$ and an Ion cutoff of 48. Three replicates were analyzed and 138 proteins found to be in common between two of the three replicates. Using these 138 proteins, we searched the literature to identify which of these proteins are known to interact with PRRs.

Flow cytometery analysis

50,000 HMVECs were seeded into 35 mm Biocoat (Corning) plates. Media was changed every day and on Day 3 postseeding the growth media was removed and replaced with 1.5 mL of basal EBM-2 media or necrotic supernatant. Cells were placed back in the incubator for 16 h and then FACS analysis performed. For intracellular proteins, cells were fixed for 15 min at 37°C using 1 mL BD Cytofix Fixation Buffer (BD Biosciences) then permeabilized with Perm Wash Buffer (Biolegend) according to manufacturer's instructions. For extracellular staining, cells were not fixed and 1:100 Fc block (Biolegend) was applied for 5 min before staining. Antibodies were used at a final dilution of 1:100. NOD1-Alexa Fluor 750 was purchased from Novus Biologics. NOD2-mouse IgG1 was from Santa Cruz, clone 2D9 followed by antimouse IgG1 AlexaFluor 488 (Biolegend). NLRP3-APC was from R&D systems. TLR2-PE and TLR4-BV421 were from Biolegend.

qPCR

HMVECs were seeded at a concentration of 100,000 cells per well into 12 well plates. Media was changed every day and stimulated 48 h after seeding. Growth media was removed and replaced with 1000 μL of EBM-2 control media and cells placed back in incubator for 1 h to quiesce. After 1 h, EBM-2 media was removed and replaced with 500 μL of EBM-2 control or necrotic

supernatant. Cells were placed in incubator for 3 h, washed x2 with 2 mL room temperature PBS then lysed with 300 μL of RNA lysis buffer (Zymo Research). Lysates were stored at −80°C until analysis was performed.

RNA was created using the Zymo Research Quick RNA mini prep (Zymo Research), according to the manufacturer's instructions. cDNA was created using the SuperScript III First Strand Synthesis System (Thermo Fisher). cDNA concentrations were standardized to 200 ng/μL using DPEC-treated water (Thermo Fisher). All primers were purchased from Genecopoeia. Master mix was created using the following formula: 1 μL primer + 5 μL PowerUp SYBR green master mix (Thermo Fisher). 6 μL of this master mix was added to 4 μL of cDNA in a 96-well PCR reaction plate (Thermo Fisher). Quantitative reverse-transcription polymerase chain reaction (RT-qPCR) was then run on a Quant Studio 3 Real-Time PCR system (Thermo Fisher). Reactions were run in triplicates. Data was analyzed on the Quant Studio software. GAPDH was used as a housekeeping gene.

RNA seq

Cells were stimulated and RNA isolated as described under qPCR. Total RNA samples were prepared into RNAseq libraries using the NEBNext Ultra Directional RNA Library Prep Kit for Illumina following manufacturer's recommended protocol. Briefly, for each sample 500 ng total RNA was polyA selected, converted to double-stranded cDNA followed by fragmentation and ligation of sequencing adapters. The library was PCR amplified 12–15 cycles using barcoded PCR primers, purified and size selected using AMPure XP Beads and loaded onto an Illumina NextSeq. 2000 for 100 base single read sequencing at an average of 61 million reads per sample (range 54–68 million reads). The data analysis was conducted using a custom RNA-seq pipeline for alignment with STAR to the Hg38 reference genome and read quantification using Salmon to estimate the abundance of transcripts. Differential gene expression analysis was carried out using edgeR. Pathway analysis was done using Advaita iPathway guide (Advaitabio).

Luminex for cell signaling molecules

HMVECs were seeded at a concentration of 85,000 cells per well into 12 well plates. Media was changed every day and stimulated 72 h after seeding. Growth media was removed and replaced with 1000 μL of EBM-2 basal media and cells placed back in incubator for 1 h to quiesce. After 1 h, EBM-2 media was removed and replaced with 500 μL of EBM-2 control or necrotic supernatant. Cells were placed in incubator for indicated time points, washed x2 with 2 mL room temperature PBS then lysed with 300 μL of protein lysis buffer. Lysates were stored at −80°C until analysis was performed and then standardized to 200 μg/mL total protein. Phospho-proteins were detected using the Bio-Rad MAPK 9plex cell signaling kit (Bio-Rad), and Millipore NF-kb 6plex assay (Millipore) according to the manufacturer's instructions. The fluorescence was standardized using β-actin (Bio-Rad) or GAPDH (Millipore). The units are presented as units of phosphorylated-protein fluorescence/β-actin or GAPDH fluorescence.

Luminex for cytokine levels

HMVECs were seeded at a concentration of 50,000 cells per well into 24-well plates. Media was changed every day and stimulated 72 h after seeding. Growth media was removed and replaced with 400 μL of EBM-2 control or necrotic supernatant. 400 μL of necrotic supernatant was added to a separate well that contained no cells to act as an internal control. Cells were placed in the incubator (37°C, 5% CO_2) for designated time points, washed two times with 2 mL room temperature PBS then lysed with 150 μL of protein lysis buffer. Lysates were stored at −80°C until analysis was performed. Lysates were tested for protein content and then analyzed using a Procarta-Plex Luminex panel (Thermo Fisher) according to the manufacturer's instructions. Analytes were measured using the BioPlex Magpix instrument (BioRad),

Endothelial permeability assay

HMVEC permeability was measured via fluorescein isothiocyanate (FITC)-dextran movement through a permeable support chamber as has been described previously.[33] 3 μm pore size permeable supports (Falcon) were placed into a 24-well plate and coated with 1:3 diluted Matrigel (BD Biosences) in DMEM:F12 (Gibco). The diluted Matrigel was quickly removed and the support chamber allowed to dry at room temperature for 15 min. 100,000 HMVECs in 500 μL of growth media were then placed in the upper chamber of each well. 800 μL of growth media was placed in the lower chamber. The media was changed the following day. Two days postseeding, the media was removed and replaced with EBM-2 basal media or necrotic supernatant (400 μL in upper chamber, 700 μL in lower chamber). Cells were placed in the incubator for 24 h after which point the upper chamber was placed into fresh wells containing

1200 µL of prewarmed EBM-2 basal media. 500 µL of 20 µg/mL of 4 kDalton FITC-dextran (Sigma), diluted in EBM-2, was then added to the upper chamber and the cells returned to the incubator for 4 h. Fluorescent intensity of the lower chamber was then measured at 485 nm excitation and 535 nm emission.

NOD inhibitor assay

25,000 HMVECs were seeded into 24-well plates in triplicate. Media was changed every day and experiments performed on Day 3 postseeding. Growth media was removed and replaced with 400 µL of prewarmed EBM-2 basal media or NOD inhibitors diluted in EBM-2. NOD1 inhibitor was 10uM Nodinitib-1 and NOD2 inhibitor was 20 µM GSK717 (MedChemExpress). Cells were placed back in the incubator for 90 min and then stimulated with 1:4 diluted necrotic supernatant in the presence or absence of inhibitor for 12 h. After 12 h, supernatant was removed and ELISA performed on the supernatant for IL6, IL8, and MCP1. 1:4 diluted necrotic supernatant was added to wells not containing cells and the absorbance of this control well was subtraced from the absorbance of any wells containing necrotic supernatant to adjust for any cytokines already present in the necrotic supernatant.

3-(4,5-Dimethyl-2-thiazolyl)-2,5-diphenyl-2H-tetrazolium bromide (MTT) assay for HMVEC viability

HMVECs were seeded in 200 µL of growth media into a 96-well Biocoat (Corning) plate (5000 cells per well for NOD1 inhibitor experiment, 10,000 cells per well for NOD2 inhibitor experiment). Media was changed the following day. Two days after seeding, growth media was removed and replaced with 200 µL of EBM basal media or inhibitor at the stated concentrations. Cells were placed back in the incubator overnight and MTT assay was then performed using the Promega CellTiter 96 MTT assay according to manufacturer instructions.

Statistics

The number of replicates for each experiment is stated in the figure legends. A student's T-test was used to compare treatments, and a p value of < 0.05 was considered significant. In the comparisons between groups for RNA sequencing, a fold change cutoff corrected for multiple testing using the Benjamini–Hochberg correction for false discovery rate of greater than 1.25 was applied. Pathways were also corrected for false discovery rate using a q-value cutoff of 0.05.
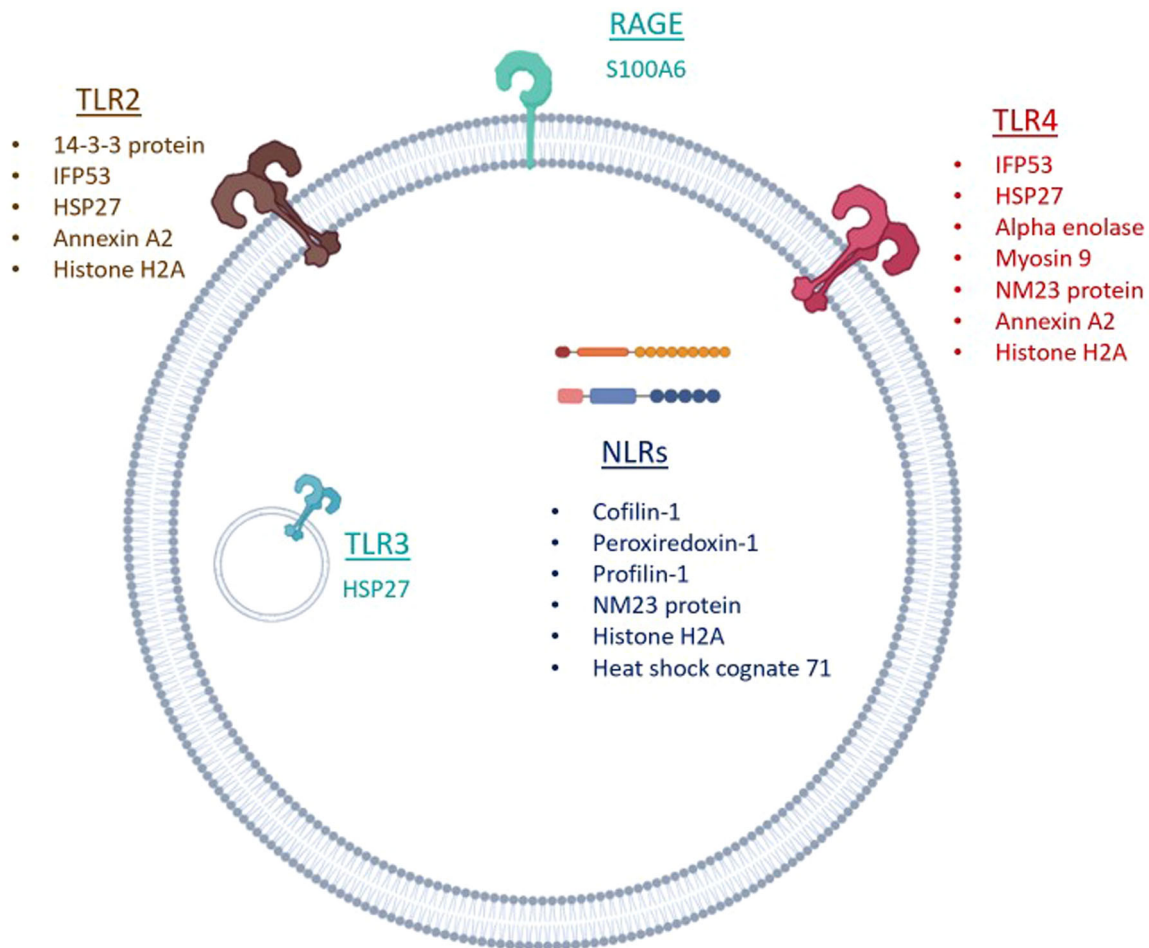
RESULTS

Necrotic supernatant derived from injured RTECs contains DAMPs

We have previously shown that necrotic supernatant from injured RTECs contains heat shock proteins and pro-inflammatory cytokines.[16] We now tested whether DAMPs known to stimulate PRRs that we and others have established play a key role in AKI [23,24,26–28,34–37] are also present in necrotic supernatant from injured RTECs. RTECs were treated with reactive oxygen species via xanthine oxidase/hypoxanthine, lysed via freeze-thaw cycles, and then mass spectrometry performed on the lysate. Screening via an unbiased approach revealed 11 proteins which are known to interact with PRRs. Each DAMP is listed underneath the PRR with which it interacts (Figure 1).[38–54] A complete list of all proteins identified is available in Supporting Information S3: Table 1.

Supernatant from injured RTECs activates genes in the NLR and TLR signaling pathways

NOD-like receptors (NLRs) and toll-like receptors (TLRs) are present in pulmonary endothelial cells and are known to signal in response to DAMPs.[8,12–14,55] We, therefore, asked whether genes in the NLR or TLR signaling pathways were differentially expressed in pulmonary HMVECs that were stimulated with supernatant from injured RTECs. Using bulk RNA sequencing we found a total of 2785 differentially expressed genes between HMVECs treated with necrotic supernatant vs media alone (Figure 2a). Each dot represents a differentially expressed gene, with blue dots representing downregulated genes and red dots representing upregulated genes. Degree of upregulation or downregulation is represented by log fold change (LogFC) on the x axis. We used Advaita iPathway® software analysis to identify biological pathways that were enriched by stimulation with necrotic supernatant. We found that 46 genes in the NLR signaling pathway (Figure 2b) and 23 genes in the TLR signaling pathway were differentially expressed (Figure 2c), suggesting that NLRs and TLRs may be involved in the HMVEC response to DAMPs derived from RTECs.

FIGURE 1 Necrotic supernatant from primary RTECs contains DAMPs that interact with PRRs. Mass spectrometry was performed on necrotic supernatant generated from injured RTECs. Protein hits were screened for previously described DAMPs. DAMPs are listed next to the PRR with which they have been reported to interact. DAMPs, damage-associated molecular patterns; HSP, heat shock protein; IFP53, tryptophanyl-tRNA synthetase; NLR, nod-like receptor; NM23, nonmetastatic protein 23; RAGE, receptor for advanced glycation endproducts; RTECs, renal tubular epithelial cell; TLR, toll-like receptor. Created using BioRender®.

Supernatant from injured RTECs causes upregulation of NOD2 and TLR2 in HMVECs

Given our findings that necrotic supernatant caused upregulation of NLR and TLR related genes in HMVECs, we next asked whether necrotic supernatant could affect PRR expression in HMVEC cells. HMVECs stimulated with necrotic supernatant had a marked increase in mRNA expression for TLR2, while TLR4 expression remained unchanged. NOD1 mRNA expression was unchanged while NOD2 mRNA expression increased signifcantly (Figure 3a). FACS analysis was performed to determine upregulation of PRRs at the protein level (Figure 3b). TLR2 expression was increased in HMVECs treated with necrotic supernatant, matching the mRNA trend. TLR4 protein expression was minimal, both at baseline and when stimulated with necrotic supernatant. There was significant baseline NOD1 expression but no observed increase with necrotic supernatant

stimulation. NOD2 protein level was minimal and similar between the two groups despite the substantial increase seen in NOD2 mRNA, suggesting a complex transcriptional regulation that will be explored in future studies. NLRP3 was highly expressed at baseline but did not change significantly when HMVECs were stimulated with necrotic supernatant.

Necrotic supernatant activates MAPKs and NFkB

Ligation of PRRs induces inflammation and cell death through a cascade of signaling events induced by mitogen-activated protein kinases (MAPKs) such as p38, ERK, and JNK.[56] We asked whether necrotic supernatant from injured RTECs activated MAPK signaling and NFkB phosphorylation in HMVECs. As shown in Figure 4, ERK1/2 as well as its upstream

(a)
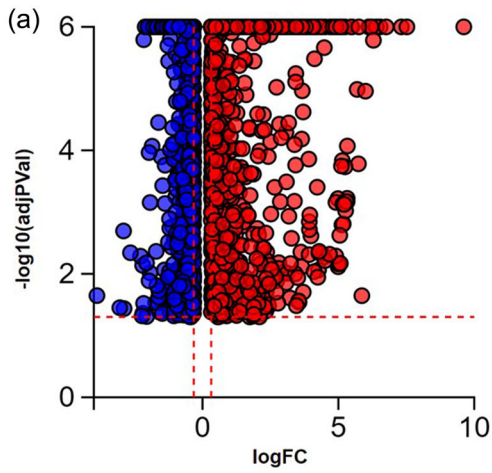
(b)

NOD like receptor pathway

(c)
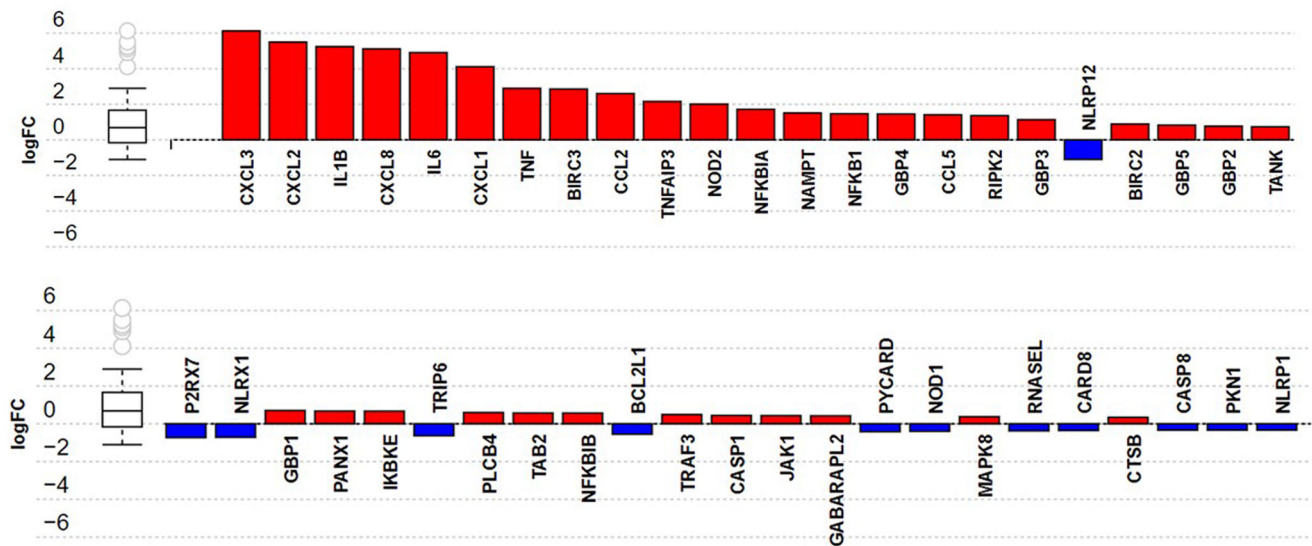
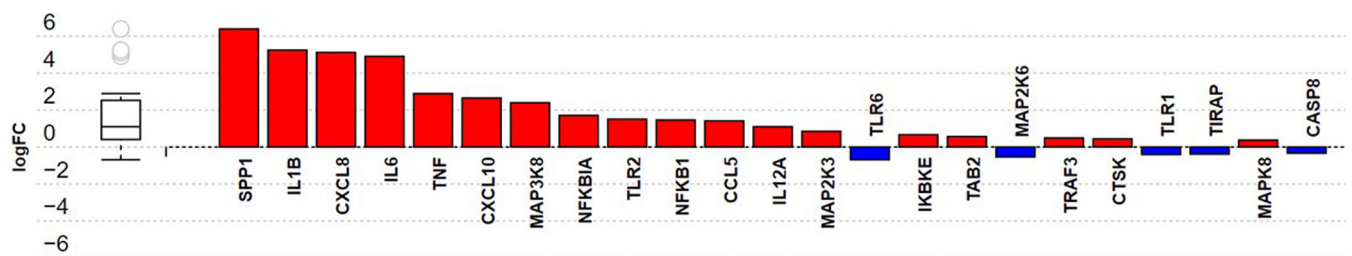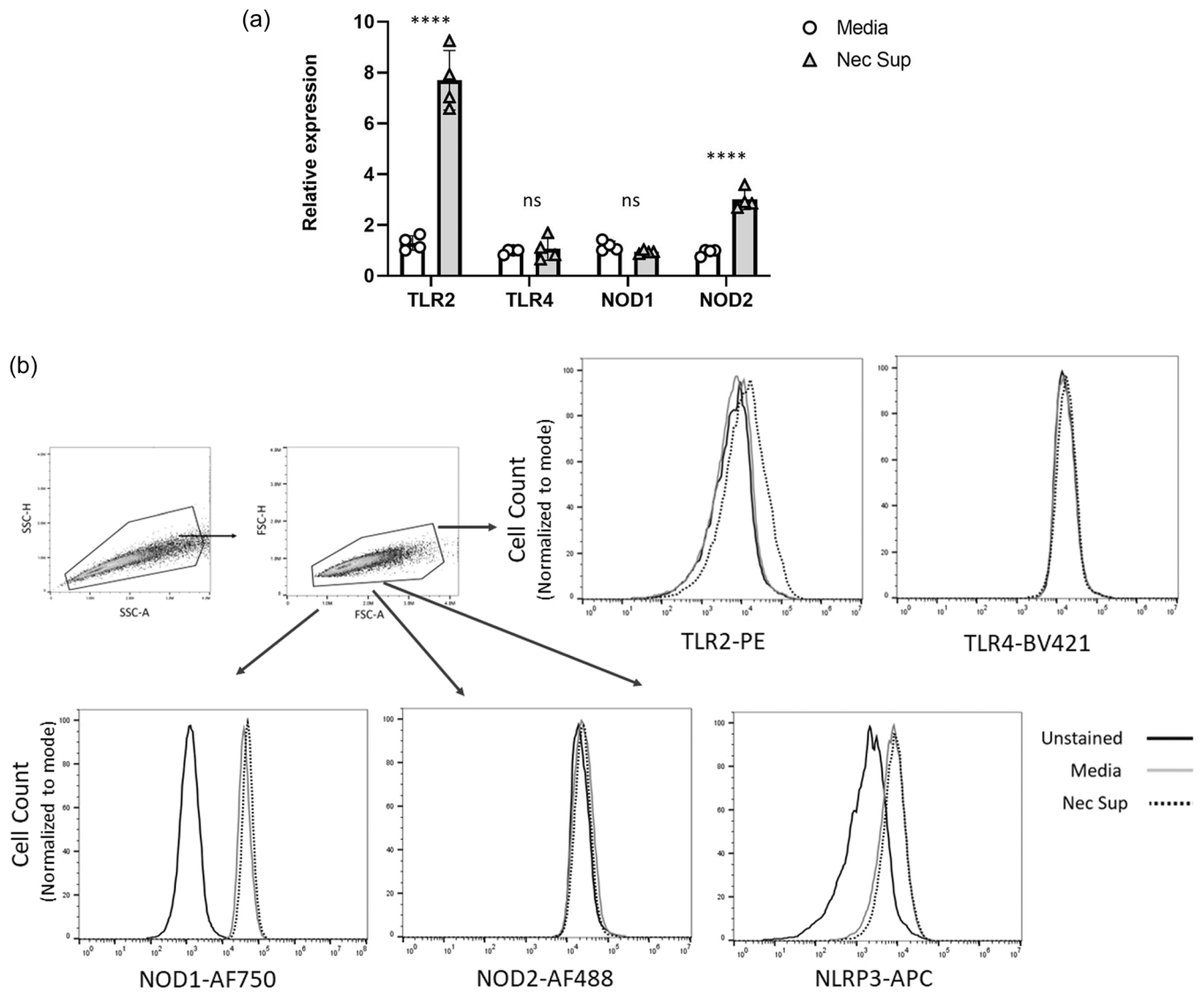## Toll like receptor pathway

FIGURE 2 (See caption on next page).

FIGURE 3 (a) Necrotic supernatant derived from renal tubular epithelial cells causes upregulation of TLR2 and NOD2 mRNA in HMVEC. Primary human microvascular endothelial cells were stimulated with media vs necrotic supernatant for 3 h and PRR mRNA upregulation measured via qPCR. Error bars represent standard deviation. $N = 4$. (b) Necrotic supernatant causes upregulation of TLR2 protein. HMVEC were stimulated with media versus necrotic supernatant and then PRR expression measured via FACS. Histograms are representative of three separate experiments. Solid black line indicates unstained cells. Solid grain line indicates stained cells that were treated with media. Dashed line indicates stained cells treated with DAMPs from injured RTECs. FACS, fluorescence activated cell sorting; HMVECs, human primary pulmonary microvascular endothelial cells; PRR, pattern recognition receptor; qPCR, quantitative polymerase chain reaction; TLRs, toll-like receptors.

FIGURE 2 Necrotic supernatant from renal tubular epithelial cells causes activation of NLR and TLR signaling pathways in HMVECs. HMVECs were stimulated for 3 h with necrotic supernatant or media and bulk RNA seq performed on cell lysates. Raw data was run through Advaita Pathway Analysis software and biologically relevant pathways with differentially expressed genes were analyzed. (a) 2785 significantly differentially expressed (DE) genes are represented in terms of their measured expression change (x-axis) and the significance of the change (y-axis). (b) Differentially expressed genes in the NOD-like receptor, and (c) toll-like receptor signaling pathways are displayed with upregulation in red and downregulation in blue. HMVECs, human primary pulmonary microvascular endothelial cells; NLRs, NOD-like receptors; TLRs, toll-like receptors.
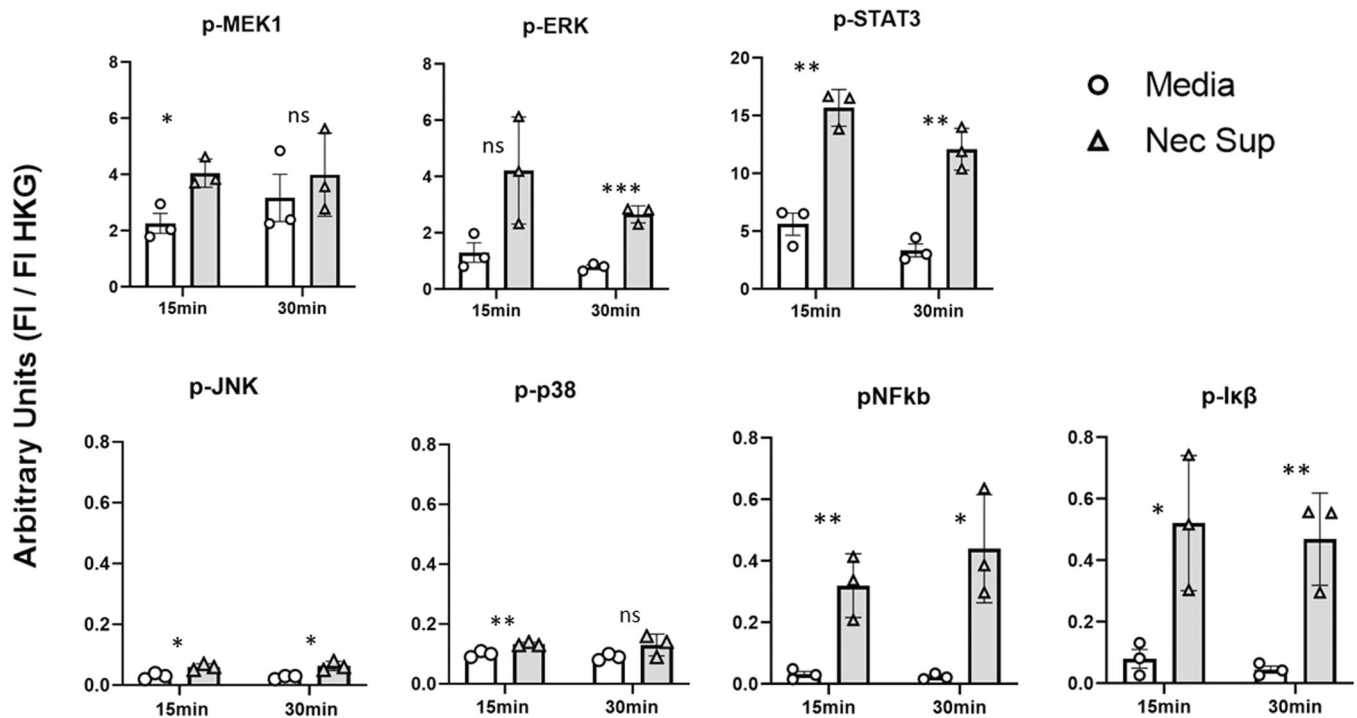
FIGURE 4 Necrotic supernatant derived from renal tubular epithelial cells causes activation of MAP kinase and NFkb signaling pathways in HMVEC. Primary human microvascular endothelial cells were quiesced for 1 h by replacing growth media with basal media without growth factors and then stimulated with basal media vs necrotic supernatant for the indicated time points. Cells were washed twice with PBS and then immediately lysed in the plate. Phosphorylated MAP kinases and NFkb pathway proteins were analyzed using Luminex. Data is presented as fluorescent intensity of phosphorylated protein divided by the fluorescent intensity of a housekeeping gene that was used as a loading control (either GAPDH or beta actin). p values represent media versus necrotic supernatant. $N = 3$. Error bars represent standard deviation. HMVECs, human primary pulmonary microvascular endothelial cells; MAP, mitogen-activated protein.

regulator MEK1 were activated by necrotic supernatant. The transcription factor Signal Transducer and Activation of Transcription 3 (Stat3), which is downstream of ERK,[57] was also significantly induced in HMVECs exposed to RTEC DAMPs. There was a statistical difference in JNK and p38 activation, but the absolute differences were negligible. We also tested for NFkB pathway activation and found that NFkB as well as its upstream regulator IkB were significantly induced when stimulated with necrotic supernatant. These results suggest that the MAPK response to renal derived DAMPs in HMVECs does not involve the MAPKs JNK and p38, but does involve ERKs.

HMVECs produce pro-inflammatory cytokines and upregulate cell adhesion molecules in response to necrotic supernatant from injured RTECs

Microvascular inflammation is a hallmark of ARDS and contributes to respiratory failure by contributing to fluid leak into the alveolar space.[58] We tested whether

HMVECs produced inflammatory mediators in response to necrotic supernatant and found that HMVECs stimulated over time produced significantly more IL6, IL8, MCP1, and GM-CSF compared to media alone as well as a nonsignificant increase in MIP1β expression. We did not observe a significant increase in TNFa (Figure 5a). We also analyzed HMVECs for expression of selectins and adhesions molecules. We found a significant increase in E-Selectin after stimulation with necrotic supernatant and a nonstatistically significant increase in P-selectin. There was also an increase in VCAM expression at 6 h post stimulation, but this result was not statistically significant (Figure 5b).

Necrotic supernatant from injured RTECs causes increased permeability in pulmonary HMVECs

We investigated whether exposure to RTEC-derived DAMPs enhanced HMVEC permeability using a FITC-dextran-based model. This model measures FITC-dextran movement through an HMVEC monolayer from the upper chamber

(a)

(b)
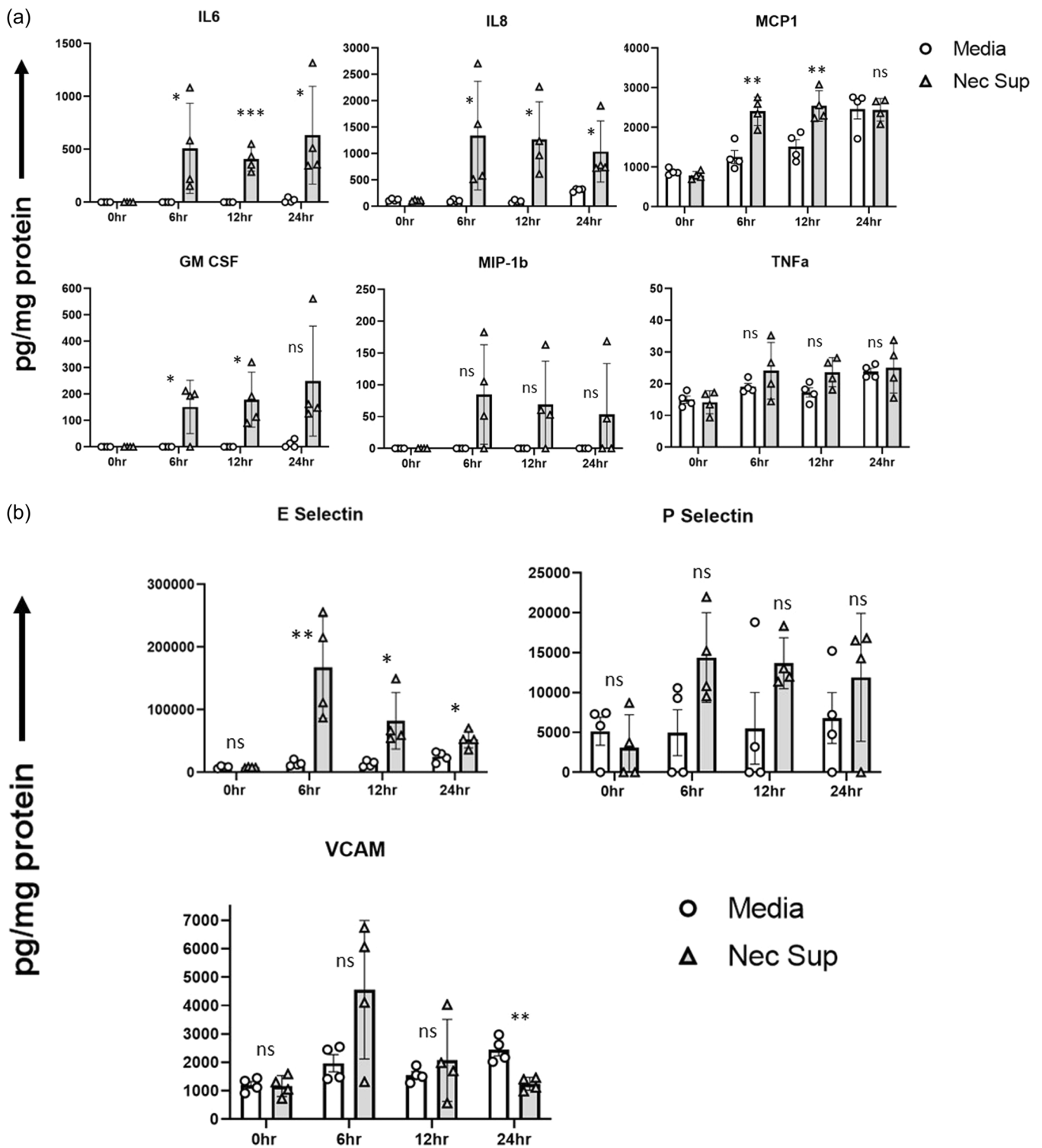
FIGURE 5 Necrotic supernatant derived from renal tubular epithelial cells causes increased (a) cytokine and (b) adhesion molecule expression in pulmonary HMVECs. HMVECs were stimulated for indicated time points with media versus necrotic supernatant. Cells were washed then lysed in the plate. Cytokines and adhesion molecules were measured via Luminex and values standardized to total protein content. $N = 4$. p values represent necrotic supernatant versus media for each time point. HMVECs, human primary pulmonary microvascular endothelial cells.
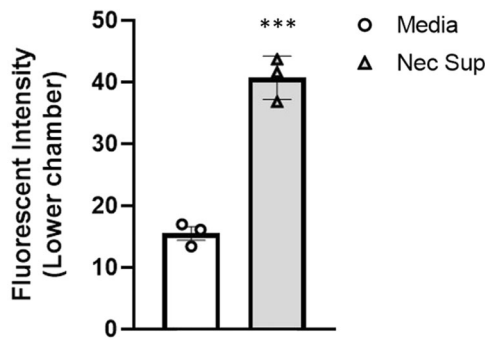
FIGURE 6 Necrotic supernatant derived from renal tubular epithelial cells causes increased permeability in HMVECs. HMVEC cells were seeded into the upper chamber of a 3-μm pore permeable support chamber to create a confluent monolayer. Cells were then stimulated with media versus necrotic supernatant for 24 h and then permeability measured via translocation of FITC-dextran into the lower chamber. Data is presented as fluorescent intensity of FITC in the lower chamber. Experiments were run in triplicate. Graph represents three separate experiments. Error bars represent standard deviation. FITC, fluorescein isothiocyanate; HMVECs, human primary pulmonary microvascular endothelial cells.

of a permeable support chamber into the lower chamber. HMVECs were stimulated for 24 h in media or necrotic supernatant and FITC-dextran permeability was measured using a fluorometer. HMVECs treated with necrotic supernatant had significantly greater permeability than those treated with media alone (Figure 6).

Inhibition of NOD1 or NOD2 decreases cytokine production in HMVECs treated with necrotic supernatant

Because we saw differential expression of genes in the NLR signaling pathways in response to RTEC DAMPs, we next asked whether inhibition of NOD1 or NOD2 influenced pro-inflammatory cytokine production in HMVECs stimulated with necrotic supernatant from injured RTECs. HMVECs were stimulated for 12 h in the presence or absence of NOD1 and NOD2 inhibitors (Nodinitib-1 10 μM and GSK717 20 μM, respectively) and the supernatant assessed for secreted cytokines. We found that NOD2 inhibition caused significantly less IL-6, IL-8, and MCP-1 production, and NOD1 inhibition caused significantly less IL-6 and MCP-1 production when compared with HMVECs stimulated without inhibitors (Figure 7a). We performed an MTT assay to ensure that the inhibitors were not affecting cell viability and found that neither the NOD1 nor the NOD2 inhibitor caused an increase in cell death (Figure 7b).

DISCUSSION

Lung injury following AKI increases mortality and the molecular mechanisms behind kidney/lung interaction remain poorly understood. In the current study, we have shown that DAMPs generated from primary human RTECs cause PRR upregulation, inflammatory cytokine production, cell signaling activation, and increased permeability in primary human microvascular endothelial cells. We chose to focus on microvascular endothelial cells because these cells have high exposure to circulating DAMPs and are critical for the pathogenesis of ARDS.[59] The lung receives 100% of the cardiac output, all of which is traveling through slow-moving capillary networks. This slow-moving blood increases the chances of DAMP-PRR interaction, making the lung particularly susceptible to any renal-derived DAMPs that may be in the circulation.

The study employs human primary renal tubular epithelial cells for the derivation of damage-associated molecular patterns, and as such offers an opportunity to investigate the impact of RTEC-derived DAMPs on *human* primary microvascular endothelial cells. Previous studies of lung injury after AKI have used renal ischemia–reperfusion models in mice[19,60–64] or serum derived from rodents who have undergone AKI to treat pulmonary endothelial cells.[17,21] Our study adds to the understanding of kidney–lung interaction as it shows that *human* pulmonary microvascular cells respond to DAMPs derived from *human* renal tubular cells.

Our data also add to our understanding of PRR expression in human pulmonary microvascular endothelial cells. There are very few reports that we are aware of which show definitive expression of NLRP3 and TLR2 in human pulmonary MVECs [14,65–67] and the only available data regarding NOD1 and NOD2 in pulmonary HMVECs is based on response to synthetic ligands rather than protein expression.[8] Our data show expression of TLR2, NOD1, and NLRP3 protein, which suggests future work may benefit from focus on these PRRs. There was a trend towards downregulation of NOD1 in the necrotic supernatant group in our RNA seq data, which is the opposite of what we had expected. However, the qPCR data showed no significant difference between media and necrotic supernatant. qPCR is more accurate than RNA seq to detect small changes in mRNA expression, so we believe the qPCR data is more reflective of the true transcriptional changes, or lack thereof. However, this trend is intriguing, especially in the context of our NOD1 inhibitor data, and this finding will be further explored in our future work.

We found that necrotic supernatant from renal tubular epithelial cells caused activation of specific
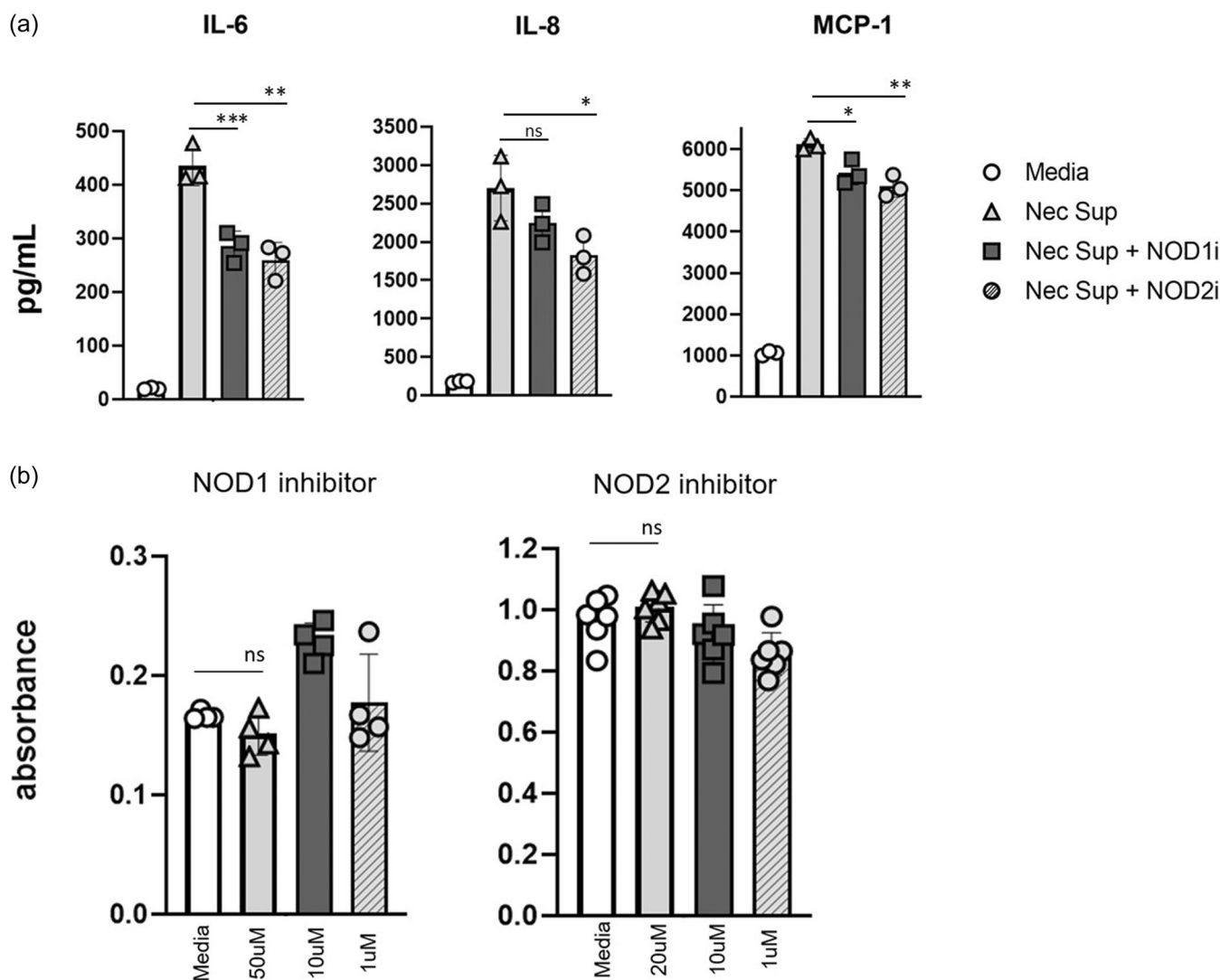
FIGURE 7 (a) Inhibition of NOD1 or NOD2 decreases cytokine secretion in response to necrotic supernatant. HMVECs were stimulated with necrotic supernatant for 12 h in the presence or absence of NOD1 (10 μM Nodinitib-1) and NOD2 inhibitor (20 μM GSK717). IL6, IL8, and MCP1 were then measured in the cell supernatant. Experiments were run in triplicate. Graph is representative of three separate experiments. Error bars represent standard deviation. p values are in comparison to necrotic supernatant without inhibitors. (b) MTT assay measuring HMVEC viability in the presence of basal media versus varying concentrations of NOD1 and NOD2 inhibitor. Absorbance is directly proportional to the number of viable cells. HMVECs, human primary pulmonary microvascular endothelial cells; IL, interleukin;MTT, 3-(4,5-dimethyl-2-thiazolyl)-2,5-diphenyl-2H-tetrazolium bromide.

MAP kinase pathways, namely the MEK/ERK pathway. This specificity is similar to what we have reported in renal tubular epithelial cell response to necrotic supernatant,[16] indicating there may be a common cell signaling pathway between the two cell types. This has implications for developing therapeutics if a shared putative pathway could be identified, given that the ideal treatment would target both sides of the kidney-lung axis.

We have also shown that inhibition of NOD1 and NOD2 ameliorates the IL-6 response to necrotic supernatant, which suggests that NOD1/2 may be a

therapeutic target in kidney-lung crosstalk. Klein et al. showed that IL-6 knockout mice were highly protected from acute lung injury following ischemic kidney injury, despite equivalent degrees of AKI between the two groups.[63] The findings from Klein et al. suggest that IL-6 signaling in the lung is critical to the response to AKI and that lung-specific treatments targeting IL-6 may have therapeutic benefit. Furthermore, anti-IL-6 therapies have been used in patients with ARDS and have been associated with lower 28-day mortality.[68] In this context, our finding that NOD1/2 inhibition in pulmonary HMVECs protects against IL6 production is particularly

important. IL-6 is also known to be downstream of NOD signaling,[69,70] which adds biologic plausibility to our findings. We chose to focus on NOD1/NOD2 inhibition in our study because TLR2 signaling involves a complex set of co-receptors/regulators. To appropriately study the effect of TLR2 inhibition would require much more complex procedures involving inhibition of TLR1, TLR6, and/or CD14.[71] Cooperation with TLR4 and TLR2 is also described [72,73] which adds a level of complexity to these types of studies. The effect of TLR2 inhibition on response to necrotic supernatant is an area of active research in our lab and will be the focus of future studies.

Our study has some limitations that should be noted. The ex vivo model is naturally limited by the lack of in vivo dynamics. Injection of necrotic supernatant into humans is not possible and injection into the mouse circulation would be biased by xenogeneic immune responses. Therefore, we believe our model is a reasonable approach for studying the effect of human-derived DAMPs on human HMVECs. Another limitation of our study is that we do not explore which specific molecules within the necrotic supernatant are mediating the effects observed in the HMVECs. We have characterized which proteins are found in the necrotic supernatant using proteomics, but there are likely other molecules such as RNA, DNA, microRNAs, or large membrane fragments present in the necrotic supernatant that have signaling properties as well. We have not performed an exhaustive evaluation of all of these molecules because we are interested in the PRR response to DAMPs rather than the individual DAMPs themselves. We focus on PRR signaling in the target cell rather than trying to identify specific DAMPs for for two reasons: (1) PRRs can bind multiple DAMPs, which suggests that therapeutic inhibition of PRRs may have a larger effect than blockade of a single DAMP; and (2) studying the effect of individual DAMPs requires the use of germ-free mice and germ-free conditions and is impractical for long term studies. Another limitation of our model is possible off-target effects and lack of specificity of the NOD1 and NOD2 inhibitors. However, the development of these inhibitors demonstrated high specificity to NOD1 [74] and NOD2 [75] with no observed off-target effects, and these inhibitors have been used in many other publications to investigate the roles of NOD1 [76–83] and NOD2.[84–86]

In summary, the data demonstrate that human primary microvascular endothelial cells respond to DAMPs derived from renal tubular epithelial cells and that PRRs known to be important in AKI are present in HMVEC and are involved in the response to these DAMPs. This work adds to the understanding of the mechniasms of kidney-lung crosstalk and provides a model for future studies aimed at developing therapeutics that may provide benefit during acute lung injury and multiorgan failure.

AUTHOR CONTRIBUTIONS

Sean E. DeWolf participated in research design, performance of the research, writing of the article, and data analysis. Alana A. Hawkes participated in performance of the research, writing of the article, and data analysis. Sunil M. Kurian participated in writing of the article and data analysis. Diana E. Gorial participated in performance of the research and writing of the article. Mark L. Hepokoski participated in writing of the article and data analysis. Stephanie S. Almeida participated in performance of the research and writing of the article. Isabella R. Posner participated in performance of the research. Dianne B. McKay participated in research design, writing of the article, and data analysis.

ACKNOWLEDGMENTS

CONFLICT OF INTEREST STATEMENT

The authors declare no conflict of interest.

ETHICS STATEMENT

None declared.

ORCID

Sean E. DeWolf http://orcid.org/0000-0001-8486-5885
Stephanie S. Almeida http://orcid.org/0000-0002-7401-2480

REFERENCES

1. Herrlich A. Interorgan crosstalk mechanisms in disease: the case of acute kidney injury-induced remote lung injury. FEBS Lett. 2022;596(5):620–37.
2. Komaru Y, Bai YZ, Kreisel D, Herrlich A. Interorgan communication networks in the kidney–lung axis. Nature Reviews. Nat Rev Nephrol. 2023;20:120–36.
3. Lee SA, Cozzi M, Bush EL, Rabb H. Distant organ dysfunction in acute kidney injury: a review. Am J Kidney Dis. 2018;72(6):846–56.
4. Chao C-T, Hou C-C, Wu V-C, Lu HM, Wang CY, Chen L, Kao TW. The impact of dialysis-requiring acute kidney injury on long-term prognosis of patients requiring prolonged mechanical ventilation: nationwide population-based study. PLoS One. 2012;7(12):e50675.
5. Ko GJ, Rabb H, Hassoun HT. Kidney-lung crosstalk in the critically ill patient. Blood Purif. 2009;28(2):75–83.
6. Thakar CV, Christianson A, Freyberg R, Almenoff P, Render ML. Incidence and outcomes of acute kidney injury

in intensive care units: a veterans administration study. Crit Care Med. 2009;37(9):2552–8.

7. Doi K, Ishizu T, Tsukamoto-Sumida M, Hiruma T, Yamashita T, Ogasawara E, Hamasaki Y, Yahagi N, Nangaku M, Noiri E. The high-mobility group protein B1-Toll-like receptor 4 pathway contributes to the acute lung injury induced by bilateral nephrectomy. Kidney Int. 2014;86(2):316–26.

8. Gatheral T, Reed DM, Moreno L, Gough PJ, Votta BJ, Sehon CA, Rickard DJ, Bertin J, Lim E, Nicholson AG, Mitchell JA. A key role for the endothelium in NOD1 mediated vascular inflammation: comparison to TLR4 responses. PLoS One. 2012;7(8):e42386.

9. Hepokoski M, Singh P. Mitochondria as mediators of systemic inflammation and organ cross talk in acute kidney injury. Am J Physiol-Renal Physiol. 2022;322(6):F589–96.

10. Hepokoski M, Wang J, Li K, Li Y, Gupta P, Mai T, Moshensky A, Alotaibi M, Crotty Alexander LE, Malhotra A, Singh P. Altered lung metabolism and mitochondrial DAMPs in lung injury due to acute kidney injury. Am J Physiol-Lung Cell Mol Physiol. 2021;320(5):L821–31.

11. Hepokoski ML, Bellinghausen AL, Bojanowski CM, Malhotra A. Can we DAMPen the cross-talk between the lung and kidney in the ICU? Am J Respir Crit Care Med. 2018;198(9):1220–2.

12. Vlacil AK, Vollmeister E, Bertrams W, Schoesser F, Oberoi R, Schuett J, Schuett H, Huehn S, Bedenbender K, Schmeck BT, Schieffer B, Grote K. Identification of microRNAs involved in NOD-dependent induction of pro-inflammatory genes in pulmonary endothelial cells. PLoS One. 2020;15(4): e0228764.

13. Wilhelmsen K, Mesa KR, Prakash A, Xu F, Hellman J. Activation of endothelial TLR2 by bacterial lipoprotein upregulates proteins specific for the neutrophil response. Innate Immun. 2011;18(4): 602–16.

14. Xu Z, Ren R, Jiang W. The protective role of raltegravir in experimental acute lung injury in vitro and in vivo. Braz J Med Biol Res. 2022;55:e12268.

15. Zhang Y, Zhang H, Li S, Huang K, Jiang L, Wang Y. Metformin alleviates LPS-induced acute lung injury by regulating the SIRT1/NF-κB/NLRP3 pathway and inhibiting endothelial cell pyroptosis. Front Pharmacol. 2022;13:801337.

16. DeWolf SE, Kasimsetty SG, Hawkes AA, Stocks LM, Kurian SM, McKay DB. DAMPs released from injured renal tubular epithelial cells activate innate immune signals in healthy renal tubular epithelial cells. Transplantation. 2022;106(8):1589–99.

17. Feltes CM, Hassoun HT, Lie ML, Cheadle C, Rabb H. Pulmonary endothelial cell activation during experimental acute kidney injury. Shock. 2011;36(2):170–6.

18. Grams ME, Rabb H. The distant organ effects of acute kidney injury. Kidney Int. 2012;81(10):942–8.

19. Hassoun HT, Grigoryev DN, Lie ML, Liu M, Cheadle C, Tuder RM, Rabb H. Ischemic acute kidney injury induces a distant organ functional and genomic response distinguishable from bilateral nephrectomy. Am J Physiol-Renal Physiol. 2007;293(1):F30–40.

20. Kim J, Baalachandran R, Li Y, Zhang CO, Ke Y, Karki P, Birukov KG, Birukova AA. Circulating extracellular histones exacerbate acute lung injury by augmenting pulmonary endothelial dysfunction via TLR4-dependent mechanism. Am J Physiol-Lung Cell Mol Physiol. 2022;323(3):L223–39.

21. White LE, Cui Y, Shelak CMF, Lie ML, Hassoun HT. Lung endothelial cell apoptosis during ischemic acute kidney injury. Shock. 2012;38(3):320–7.

22. Zhao H, Ning J, Lemaire A, Koumpa FS, Sun JJ, Fung A, Gu J, Yi B, Lu K, Ma D. Necroptosis and parthanatos are involved in remote lung injury after receiving ischemic renal allografts in rats. Kidney Int. 2015;87(4):738–48.

23. Kim HJ, Lee DW, Ravichandran K, O. Keys D, Akcay A, Nguyen Q, He Z, Jani A, Ljubanovic D, Edelstein CL. NLRP3 inflammasome knockout mice are protected against ischemic but not cisplatin-induced acute kidney injury. J Pharmacol Exp Ther. 2013;346(3):465–72.

24. Leemans JC, Stokman G, Claessen N, Rouschop KM, Teske GJD, Kirschning CJ, Akira S, van der Poll T, Weening JJ, Florquin S. Renal-associated TLR2 mediates ischemia/reperfusion injury in the kidney. J Clin Invest. 2005;115(10):2894–903.

25. Pulskens WP, Teske GJ, Butter LM, Roelofs JJ, van der Poll T, Florquin S, Leemans JC. Toll-like receptor-4 coordinates the innate immune response of the kidney to renal ischemia/reperfusion injury. PLoS One. 2008;3(10):e3596.

26. Shigeoka AA, Holscher TD, King AJ, Hall FW, Kiosses WB, Tobias PS, Mackman N, McKay DB. TLR2 is constitutively expressed within the kidney and participates in ischemic renal injury through both MyD88-dependent and -independent pathways. J Immunol. 2007;178(10):6252–8.

27. Shigeoka AA, Kambo A, Mathison JC, King AJ, Hall WF, da Silva Correia J, Ulevitch RJ, McKay DB. Nod1 and nod2 are expressed in human and murine renal tubular epithelial cells and participate in renal ischemia reperfusion injury. J Immunol. 2010;184(5):2297–304.

28. Shigeoka AA, Mueller JL, Kambo A, Mathison JC, King AJ, Hall WF, Correia JS, Ulevitch RJ, Hoffman HM, McKay DB. An inflammasome-independent role for epithelial-expressed Nlrp3 in renal ischemia-reperfusion injury. J Immunol. 2010;185(10):6277–85.

29. Mackay LS, Dodd S, Dougall IG, Tomlinson W, Lordan J, Fisher AJ, Corris PA. Isolation and characterisation of human pulmonary microvascular endothelial cells from patients with severe emphysema. Respir Res. 2013;14(1):23.

30. Wang J, Niu N, Xu S, Jin ZG. A simple protocol for isolating mouse lung endothelial cells. Sci Rep. 2019;9(1):1458.

31. Gillich A, Zhang F, Farmer CG, Travaglini KJ, Tan SY, Gu M, Zhou B, Feinstein JA, Krasnow MA, Metzger RJ. Capillary cell-type specialization in the alveolus. Nature. 2020; 586(7831):785–9.

32. Schupp JC, Adams TS, Cosme C, Raredon MSB, Yuan Y, Omote N, Poli S, Chioccioli M, Rose KA, Manning EP, Sauler M, DeIuliis G, Ahangari F, Neumark N, Habermann AC, Gutierrez AJ, Bui LT, Lafyatis R, Pierce RW, Meyer KB, Nawijn MC, Teichmann SA, Banovich NE, Kropski JA, Niklason LE, Pe'er D, Yan X, Homer RJ, Rosas IO, Kaminski N. Integrated single-cell atlas of endothelial cells of the human lung. Circulation. 2021;144(4):286–302.

33. Martins-Green M, Petreaca M, Yao M. An assay system for in vitro detection of permeability in human "endothelium". Methods Enzymol. 2008;443:137–53.

34. Allam R, Scherbaum CR, Darisipudi MN, Mulay SR, Hägele H, Lichtnekert J, Hagemann JH, Rupanagudi KV,

Ryu M, Schwarzenberger C, Hohenstein B, Hugo C, Uhl B, Reichel CA, Krombach F, Monestier M, Liapis H, Moreth K, Schaefer L, Anders HJ. Histones from dying renal cells aggravate kidney injury via TLR2 and TLR4. J Am Soc Nephrol. 2012;23(8):1375–88.

35. Guo Y, Zhang J, Lai X, Chen M, Guo Y. Tim-3 exacerbates kidney ischaemia/reperfusion injury through the TLR-4/NF-κB signalling pathway and an NLR-C4 inflammasome activation. Clin Exp Immunol. 2018;193(1):113–29.

36. Miyagawa T, Iwata Y, Oshima M, Ogura H, Sato K, Nakagawa S, Yamamura Y, Kamikawa Y, Miyake T, Kitajima S, Toyama T, Hara A, Sakai N, Shimizu M, Furuichi K, Munesue S, Yamamoto Y, Kaneko S, Wada T. Soluble receptor for advanced glycation end products protects from ischemia- and reperfusion-induced acute kidney injury. Biol Open. 2022;11(1):PMC8822355.

37. Paulus P, Rupprecht K, Baer P, Obermüller N, Penzkofer D, Reissig C, Scheller B, Holfeld J, Zacharowski K, Dimmeler S, Schlammes J, Urbschat A. The early activation of toll-like receptor (TLR)-3 initiates kidney injury after ischemia and reperfusion. PLoS One. 2014;9(4):e94366.

38. Guillou C, Fréret M, Fondard E, Derambure C, Avenel G, Golinski ML, Verdet M, Boyer O, Caillot F, Musette P, Lequerré T, Vittecoq O. Soluble alpha-enolase activates monocytes by CD14-dependent TLR4 signalling pathway and exhibits a dual function. Sci Rep. 2016;6:23796.

39. Wu X, Xiong F, Fang H, Zhang J, Chang M. Crosstalks between NOD1 and histone H2A contribute to host defense against *Streptococcus agalactiae* infection in zebrafish. Antibiotics. 2021;10(7):861.

40. Xu J, Zhang X, Monestier M, Esmon NL, Esmon CT. Extracellular histones are mediators of death through TLR2 and TLR4 in mouse fatal liver injury. J Immunol. 2011;187(5):2626–31.

41. Nguyen TTT, Yoon HK, Kim YT, Choi YH, Lee WK, Jin M. Tryptophanyl-tRNA synthetase 1 signals activate TREM-1 via TLR2 and TLR4. Biomolecules. 2020;10(9):1283.

42. Tsai J-C, Lin Y-W, Huang C-Y, Lin CY, Tsai YT, Shih CM, Lee CY, Chen YH, Li CY, Chang NC, Lin FY, Tsai CS. The role of calpain-myosin 9-Rab7b pathway in mediating the expression of toll-like receptor 4 in platelets: a novel mechanism involved in α-granules trafficking. PLoS One. 2014;9:e85833.

43. Trova S, Fenton M, Chauhan B, Puri A, Lomada S, Adams A, Wieland T, Drayson MT, Khanim FL, Bunce CM, Lin F. Human and pathogen derived ndpks act as novel damps and PAMPs to drive leukemia cell survival and progression through signaling via the TLR4-mediated alternative NLRP3 inflammasome pathway. Blood. 2019;134:2684.

44. He Y, Li S, Tang D, Peng Y, Meng J, Peng S, Deng Z, Qiu S, Liao X, Chen H, Tu S, Tao L, Peng Z, Yang H. Circulating Peroxiredoxin-1 is a novel damage-associated molecular pattern and aggravates acute liver injury via promoting inflammation. Free Radical Biol Med. 2019;137:24–36.

45. Pazoki H, Mirjalali H, Niyyati M, Seyed Tabaei SJ, Mosaffa N, Shahrokh S, Asadzadeh Ahdaei H, Kupz A, Zali MR. Toxoplasma gondii profilin induces NLRP3 activation and IL-1β production/secretion in THP-1 cells. Microb Pathog. 2023;180:106120.

46. Bonam SR, Ruff M, Muller S. HSPA8/HSC70 in immune disorders: a molecular rheostat that adjusts chaperone-mediated autophagy substrates. Cells. 2019;8(8):849.

47. Park YH, Kastner D, Chae JJ. Cofilin-1 is an essential redox sensor for NLRP3 inflammasome activation. Pediatr Rheumatol Online J. 2015;13(Suppl 1):O52. https://doi.org/10.1186/1546-0096-13-S1-O52

48. Kadota Y, Shirasu K, Guerois R. NLR sensors meet at the SGT1-HSP90 crossroad. Trends Biochem Sci. 2010;35(4):199–207.

49. Singh P, Ali SA. Multifunctional role of S100 protein family in the immune system: an update. Cells. 2022;11(15):2274.

50. Munier CC, Ottmann C, Perry MWD. 14-3-3 modulation of the inflammatory response. Pharmacol Res. 2021;163:105236.

51. Vabulas RM, Wagner H, Schild H. Heat shock proteins as ligands of toll-like receptors. Curr Top Microbiol Immunol. 2002;270:169–84.

52. Batulan Z, Pulakazhi Venu VK, Li Y, Koumbadinga G, Alvarez-Olmedo DG, Shi C, O'Brien ER. Extracellular release and signaling by heat shock protein 27: role in modifying vascular inflammation. Front Immunol. 2016;7:285.

53. Swisher JFA, Burton N, Bacot SM, Vogel SN, Feldman GM. Annexin A2 tetramer activates human and murine macrophages through TLR4. Blood. 2010;115(3):549–58.

54. Andersen BM, Xia J, Epstein AL, Ohlfest JR, Chen W, Blazar BR, Pennell CA, Olin MR. Monomeric annexin A2 is an oxygen-regulated toll-like receptor 2 ligand and adjuvant. J Immunother Cancer. 2016;4:11.

55. Xiang M, Shi X, Li Y, Xu J, Yin L, Xiao G, Scott MJ, Billiar TR, Wilson MA, Fan J. Hemorrhagic shock activation of NLRP3 inflammasome in lung endothelial cells. J Immunol. 2011;187(9):4809–17.

56. Li D, Wu M. Pattern recognition receptors in health and diseases. Signal Transduct Target Ther. 2021;6(1):291.

57. Chung J, Uchida E, Grammer TC, Blenis J. STAT3 serine phosphorylation by ERK-dependent and -independent pathways negatively modulates its tyrosine phosphorylation. Mol Cell Biol. 1997;17(11):6508–16.

58. Ramji HF, Hafiz M, Altaq HH, Hussain ST, Chaudry F. Acute respiratory distress syndrome; a review of recent updates and a glance into the future. Diagnostics. 2023;13:1528.

59. Vassiliou AG, Kotanidou A, Dimopoulou I, Orfanos SE. Endothelial damage in acute respiratory distress syndrome. Int J Mol Sci. 2020;21(22):8793.

60. Deng J, Hu X, Yuen PST, Star RA. α-Melanocyte–stimulating hormone inhibits lung injury after renal ischemia/reperfusion. Am J Respir Crit Care Med. 2004;169(6):749–56.

61. Hoke TS, Douglas IS, Klein CL, He Z, Fang W, Thurman JM, Tao Y, Dursun B, Voelkel NF, Edelstein CL, Faubel S. Acute renal failure after bilateral nephrectomy is associated with cytokine-mediated pulmonary injury. J Am Soc Nephrol. 2007;18(1):155–64.

62. Kim DJ, Park SH, Sheen MR, Jeon US, Kim SW, Koh ES, Woo SK. Comparison of experimental lung injury from acute renal failure with injury due to sepsis. Respiration. 2006;73(6):815–24.

63. Klein CL, Hoke TS, Fang WF, Altmann CJ, Douglas IS, Faubel S. Interleukin-6 mediates lung injury following

ischemic acute kidney injury or bilateral nephrectomy. Kidney Int. 2008;74(7):901–9.

64. Kramer AA, Postler G, Salhab KF, Mendez C, Carey LC, Rabb H. Renal ischemia/reperfusion leads to macrophage-mediated increase in pulmonary vascular permeability. Kidney Int. 1999;55(6):2362–7.

65. Paul O, Tao JQ, West E, Litzky L, Feldman M, Montone K, Rajapakse C, Bermudez C, Chatterjee S. Pulmonary vascular inflammation with fatal coronavirus disease 2019 (COVID-19): possible role for the NLRP3 inflammasome. Respir Res. 2022;23(1):25.

66. Wilhelmsen K, Mesa KR, Prakash A, Xu F, Hellman J. Activation of endothelial TLR2 by bacterial lipoprotein upregulates proteins specific for the neutrophil response. Innate Immun. 2012;18(4):602–16.

67. Zhou P, Guo H, Li Y, Liu Q, Qiao X, Lu Y, Mei PY, Zheng Z, Li J. Monocytes promote pyroptosis of endothelial cells during lung ischemia-reperfusion via IL-1R/NF-κB/NLRP3 signaling. Life Sci. 2021;276:119402.

68. Domingo P, Mur I, Mateo GM, Gutierrez MM, Pomar V, de Benito N, Corbacho N, Herrera S, Millan L, Muñoz J, Malouf J, Molas ME, Asensi V, Horcajada JP, Estrada V, Gutierrez F, Torres F, Perez-Molina JA, Fortun J, Villar LM, Hohenthal U, Marttila H, Vuorinen T, Nordberg M, Valtonen M, Frigault MJ, Mansour MK, Patel NJ, Fernandes A, Harvey L, Foulkes AS, Healy BC, Shah R, Bensaci AM, Woolley AE, Nikiforow S, Lin N, Sagar M, Shrager H, Huckins DS, Axelrod M, Pincus MD, Fleisher J, Lampa J, Nowak P, Vesterbacka JC, Rasmuson J, Skorup P, Janols H, Niward KF, Chatzidionysiou K, Asgeirsson H, Parke Å, Blennow O, Svensson AK, Aleman S, Sönnerborg A, Henter JI, Horne AC, Al-Beidh F, Angus D, Annane D, Arabi Y, Beane A, Berry S, Bhimani Z, Bonten M, Bradbury C, Brunkhorst F, Buxton M, Cheng A, Cove M, De Jong M, Derde L, Estcourt L, Goossens H, Gordon A, Green C, Haniffa R, Ichihara N, Lamontagne F, Lawler P, Litton E, Marshall J, McArthur C, McAuley D, McGuinness S, McVerry B, Montgommery S, Mouncey P, Murthy S, Nichol A, Parke R, Parker J, Reyes F, Rowan K, Saito H, Santos M, Seymour C, Shankar-Hari M, Turgeon A, Turner A, van Bentum-Puijk W, van de Veerdonk F, Webb S, Zarychanski R, Baillie JK, Beasley R, Cooper N, Fowler R, Galea J, Hills T, King A, Morpeth S, Netea M, Ogungbenro K, Pettila V, Tong S, Uyeki T, Youngstein T, Higgins A, Lorenzi E, Berry L, Salama C, Rosas IO, Ruiz-Antorán B, Muñez Rubio E, Ramos Martínez A, Campos Esteban J, Avendaño Solá C, Pizov R, Sanz Sanz J, Abad-Santos F, Bautista-Hernández A, García-Fraile L, Barrios A, Gutiérrez Liarte Á, Alonso Pérez T, Rodríguez-García SC, Mejía-Abril G, Prieto JC, Leon R, Veiga VC, Scheinberg P, Farias DLC, Prats JG, Cavalcanti AB, Machado FR, Rosa RG, Berwanger O. Association between administration of IL-6 antagonists and mortality among patients hospitalized for COVID-19: A meta-analysis. JAMA. 2021;326(6):499–518.

69. Geddes K, Rubino SJ, Magalhaes JG, Streutker C, Le Bourhis L, Cho JH, Robertson SJ, Kim CJ, Kaul R, Philpott DJ, Girardin SE. Identification of an innate T helper type 17 response to intestinal bacterial pathogens. Nature Med. 2011;17(7):837–44.

70. Strober W, Murray PJ, Kitani A, Watanabe T. Signalling pathways and molecular interactions of NOD1 and NOD2. Nat Rev Immunol. 2006;6(1):9–20.

71. van Bergenhenegouwen J, Plantinga TS, Joosten LA, Netea MG, Folkerts G, Kraneveld AD, Garssen J, Vos AP. TLR2 & co: a critical analysis of the complex interactions between TLR2 and coreceptors. J Leukoc Biol. 2013;94(5):885–902.

72. Trinchieri G, Sher A. Cooperation of toll-like receptor signals in innate immune defence. Nat Rev Immunol. 2007;7:179–90.

73. Anwar MA, Basith S, Choi S. Negative regulatory approaches to the attenuation of toll-like receptor signaling. Exp Mol Med. 2013;45(2):e11-e.

74. Correa RG, Khan PM, Askari N, Zhai D, Gerlic M, Brown B, Magnuson G, Spreafico R, Albani S, Sergienko E, Diaz PW, Roth GP, Reed JC. Discovery and characterization of 2-aminobenzimidazole derivatives as selective NOD1 inhibitors. Chem Biol 2011;18(7):825–32.

75. Rickard DJ, Sehon CA, Kasparcova V, Kallal LA, Zeng X, Montoute MN, Chordia T, Poore DD, Li H, Wu Z, Eidam PM, Haile PA, Yu J, Emery JG, Marquis RW, Gough PJ, Bertin J. Identification of benzimidazole diamides as selective inhibitors of the nucleotide-binding oligomerization domain 2 (NOD2) signaling pathway. PLoS One. 2013;8(8):e69619.

76. Huang W, Gou F, Long Y, Li Y, Feng H, Zhang Q, Gao C, Chen G, Xu Y. High glucose and lipopolysaccharide activate NOD1- RICK-NF-κB inflammatory signaling in mesangial cells. Exp Clin Endocrinol Diabetes. 2016;124(8):512–7.

77. Jiang HY, Najmeh S, Martel G, MacFadden-Murphy E, Farias R, Savage P, Leone A, Roussel L, Cools-Lartigue J, Gowing S, Berube J, Giannias B, Bourdeau F, Chan CHF, Spicer JD, McClure R, Park M, Rousseau S, Ferri LE. Activation of the pattern recognition receptor NOD1 augments colon cancer metastasis. Protein Cell. 2020;11(3):187–201.

78. Lu J, Fang K, Wang S, Xiong L, Zhang C, Liu Z, Guan X, Zheng R, Wang G, Zheng J, Wang F. Anti-Inflammatory effect of columbianetin on Lipopolysaccharide-Stimulated human peripheral blood mononuclear cells. Mediators Inflamm. 2018;2018:1–8.

79. Magnuson G, Khan P, Yuan H, Brown B, Divlianska DB, Stonich D, Peddibhotla M, Su Y, Dad S, Sergienko E, Chung TDY, Roth GP, Wimer C, Diaz P, Correa RG, Reed JC. High Throughput Screening Assays for NOD1 Inhibitors - Probe 2. Probe Reports from the NIH Molecular Libraries Program. National Center for Biotechnology Information (US): Bethesda (MD); 2010.

80. Magnuson G, Khan P, Yuan H, Brown B, Divlianska DB, Stonich D, Peddibhotla M, Su Y, Dad S, Peddibhotla E, Chung TDY, Roth GP, Wimer C, Diaz P, Correa RG, Reed JC. High Throughput Screening Assays for NOD1 Inhibitors - Probe 1. Probe Reports from the NIH Molecular Libraries Program. National Center for Biotechnology Information (US): Bethesda (MD); 2010.

81. Wei X, Liu Y, Li W, Shao X. Nucleotide-binding oligomerization domain-containing protein 1 regulates inflammatory response in endometriosis. Curr Protein Pept Sci. 2022;23(2):121–8.

82. Zhang J, Fang B, Sun L, Zhang X, Liu J, Yang Y, Zhang W, Wang X, Ding Y. Roles of NOD1/Rip2 signal pathway in carotid artery remodelling in spontaneous hypertensive rats. Gen Physiol Biophys. 2022;41(1):31–42.

83. Zhu J, Zhu R, Jiang H, Li Z, Jiang X, Li F, Zhang F, Feng X, Gu J, Li N, Lei L. Adh promotes actinobacillus pleuropneumoniae survival in porcine alveolar macrophages by inhibiting CHAC2-mediated respiratory burst and inflammatory cytokine expression. Cells. 2023;12(5):696.

84. Gao J, Zhao X, Hu S, Huang Z, Hu M, Jin S, Lu B, Sun K, Wang Z, Fu J, Weersma RK, He X, Zhou H. Gut microbial DL-endopeptidase alleviates Crohn's disease via the NOD2 pathway. Cell Host Microbe. 2022;30(10):1435–49.e9.

85. Kong X, Zhang Y, Xiang L, You Y, Duan Y, Zhao Y, Li S, Wu R, Zhang J, Zhou L, Duan L. Fusobacterium nucleatum-triggered neutrophil extracellular traps facilitate colorectal carcinoma progression. J Exp Clin Cancer Res. 2023;42(1):236.

86. Limonta D, Dyna-Dagman L, Branton W, Mancinelli V, Makio T, Wozniak RW, Power C, Hobman TC. Nodosome inhibition as a novel broad-spectrum antiviral strategy against arboviruses, enteroviruses, and SARS-CoV-2. Antimicrob Agents Chemother. 2021;65(8):e0049121.

SUPPORTING INFORMATION

Additional supporting information can be found online in the Supporting Information section at the end of this article.